BJR

https://doi.org/10.1259/bjr.20200113

Received: 23 January 2020 | Revised: 18 April 2020 | Accepted: 12 May 2020

Cite this article as:
Börnert P, Norris DG. A half-century of innovation in technology—preparing MRI for the 21st century. *Br J Radiol* 2020; **93**: 20200113.

BJR 125TH ANNIVERSARY: REVIEW ARTICLE

A half-century of innovation in technology—preparing MRI for the 21st century

[1,2]PETER BÖRNERT, PhD and [3,4,5]DAVID G. NORRIS, PhD

[1]Philips Research, Hamburg, Germany
[2]Department of Radiology, LUMC, Leiden, the Netherlands
[3]Donders Institute for Brain, Cognition and Behaviour, Radboud University, Nijmegen, Netherlands
[4]Erwin L. Hahn Institute for Magnetic Resonance Imaging, University of Duisburg-Essen, Essen, Germany
[5]Magnetic Detection and Imaging, Science and Technology Faculty, University of Twente, Enschede, Netherlands

Address correspondence to: Prof Dr Peter Börnert
E-mail: *peter.boernert@philips.com*

ABSTRACT

MRI developed during the last half-century from a very basic concept to an indispensable non-ionising medical imaging technique that has found broad application in diagnostics, therapy control and far beyond. Due to its excellent soft-tissue contrast and the huge variety of accessible tissue- and physiological-parameters, MRI is often preferred to other existing modalities. In the course of its development, MRI underwent many substantial transformations. From the beginning, starting as a proof of concept, much effort was expended to develop the appropriate basic scanning technology and methodology, and to establish the many clinical contrasts (*e.g.*, T_1, T_2, flow, diffusion, water/fat, etc.) that MRI is famous for today. Beyond that, additional prominent innovations to the field have been parallel imaging and compressed sensing, leading to significant scanning time reductions, and the move towards higher static magnetic field strengths, which led to increased sensitivity and improved image quality. Improvements in workflow and the use of artificial intelligence are among many current trends seen in this field, paving the way for a broad use of MRI. The 125th anniversary of the BJR is a good point to reflect on all these changes and developments and to offer some slightly speculative ideas as to what the future may bring.

INTRODUCTION

Up until a century ago, the living human body was almost opaque to the human eye. This changed radically with the advent of medical imaging technologies, which dramatically revolutionised medicine and in particular diagnosis, but in so doing also influenced the arts, culture and indeed modern society.[1] Among these emerging technologies, MRI is now firmly established as a key modality. It is safe for the patient from the perspective of radiation exposure and offers a range of excellent soft-tissue image contrasts, covering a huge diagnostic bandwidth that supports modern medical diagnostics, making MRI an indispensable tool in diagnosis and therapy monitoring.

Born in 1973, roughly 50 years ago, MRI started with Lauterbur's pioneering idea,[2] that established a proof of principle imaging prototype. It showed early promise in the ability to differentiate between healthy and tumorous tissue via tissue specific MR relaxation parameters (T_1, T_2),[3] but at that stage had an uncertain future. This promise triggered a number of British research groups (primarily Nottingham, Hammersmith and Aberdeen) to construct first scanner prototypes, which were based on resistive magnets. However, by modern standards, the early image quality was low, and data acquisition speeds excruciatingly slow, acquiring a single echo approximately every second and scanning a few minutes for a single low-resolution image.[4] The multi-slice multi-echo spin-echo imaging sequence introduced shortly afterwards greatly improved efficiency.[5] Furthermore, it was at the time not clear whether the young MRI branch would ever achieve whole body- or high-field imaging as experienced today.[6] From the beginning, the development of MR technology was characterised by a strong interplay between basic research and hardware development. The former established the concept of k-space,[7,8] the space in which actual MR data acquisition takes place, and the underlying principles of image formation, mainly founded on Nyquist's sampling theorem and the Fourier transform, encompassing slice-selective excitation and gradient-/spin-echo-based acquisition techniques. On the hardware side, the basic system architecture was developed, which has remained conceptually largely unchanged, but has evolved

Figure 1. Schematic evolution of the MRI system. (a) Scheme of a basic single channel transmit/receive system (Tx/Rx) used for MR spectroscopy. A corresponding proton spectrum is given which can be visualised via the user interface (UI) running on the host computer of the system. Please note, human-size systems of this kind existed only as prototypes. However, the technical roots of early MR imagers were in MR spectroscopy equipment used for chemical and structural analysis. (b) Scheme of an early MRI scanner with a three-dimensional gradient system added for spatial encoding (GA denotes the three gradient amplifiers). An early human head image added[4]. (c) Basic MRI extended with parallel reception (please see the multiple Rx channels) with a Turbo Spin Echo (TSE) image obtained with an eight-channel head coil. (d) Scheme of a modern high-field MRI additionally equipped with a parallel transmission system to mainly homogenise the transmit RF field. A dual-transmit channel RF-shimmed 3T body image added for illustration. Additionally, the reconstruction is schematically highly parallelised to keep track with the increased reconstruction demands of parallel imaging and compressed sensing. So, in general, a clear trend of parallelisation becomes visible, on the reception, the transmission and the reconstruction side. Please note that the triangles represent the amplifiers present in the corresponding chains. The small black triangles denote the MR signal pre-amplifiers, whereas the big ones mark the RF amplifiers present in the Tx chain. The large grey triangles mark the gradient amplifiers.

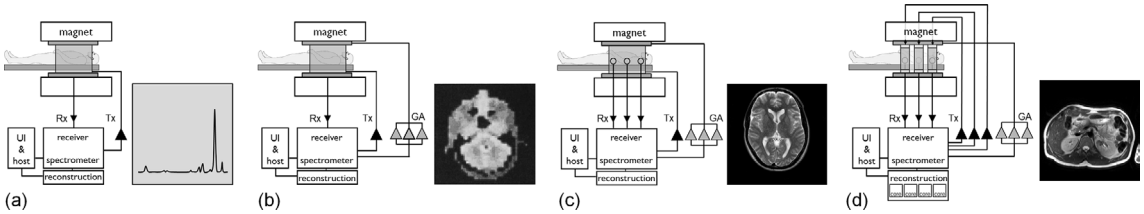

enormously in the system components and their details over the last three decades (c.f. Figure 1).

The initial systems were quite simple and consisted of a homogeneous magnet, responsible for creating the measurable polarisation within the body. The inner bore hosts a magnetic field gradient system that facilitates spatial signal encoding by allowing manipulation of a linear magnetic field, the gradient, along all three spatial axes. Within this, the antennas of the transmit and receive systems are placed, allowing excitation of the spin system and subsequent reception of the tiny MR signal responses (Figure 1b).

Since then much has changed. Hardware, methodology and clinical needs have continuously cross-fertilised each other, triggering many waves of scientific innovation, which can be grouped into several general trends:

- towards higher magnetic fields, to boost the available polarisation and thus the signal-to-noise ratio (SNR),
- to higher acquisition speed, boosting scanning efficiency, because MRI is by its nature a rather slow technique,
- towards parallelisation to increase overall system performance (including receivers, transmitters, computer cores, see Figure 1), which enabled a number of key applications,
- the quest for new diagnostic contrasts including potential biomarkers, which goes along with the trend to team up with other diagnostic modalities, like PET,[9]
- the move towards therapy where MRI acts as a camera in interventional set-ups like the MR-LINAC,[10] and
- the trend of specialisation and standardisation in the MR community. Large sub-communities and disciplines cover areas such as spectroscopy, animal research, functional MRI (fMRI) quantitative MR and interventional MRI, to name but few examples.

Although MRI may be approaching maturity, it is, and it will remain, a field of constant innovation. This will be reflected in this brief review, which aims to sketch the trajectory of selected key technical innovations of the last 30 years and to extrapolate these into the future.

FROM THE BEGINNING

MRI actually started with many challenges, as the radial imaging scheme that was initially proposed[2] gave insufficient image quality owing to the poor B_0 homogeneity of the early systems. The concept of slice selective excitation[11] which constrained the signal to a 2D plane and the introduction of Cartesian spin warp imaging[4] which uniformly samples k-space in the presence of a constant read-gradient, offered for the first time images of diagnostic quality. The simplicity and the robustness of this imaging scheme allowed also a straight-forward image reconstruction requiring only an inverse fast Fourier transform (FFT) to be applied to the sampled echo signals in k-space to yield the final images. The FFT was often run on dedicated hardware such as array processors, precursors to modern GPUs. Spin-warp is even today the dominant k-space sampling scheme, due to its straight-forward extension to 3D and high robustness to imperfections such as slight eddy currents. This paved the way for initial, clinical adoption using simple scanners, which became commercially available in the early 80s, characterised by limited speed and sequence flexibility, and offering only a small number of image contrasts (T_1 and T_2). They were operating at very low field strength,[12] with the drawback of limited SNR and limited contrast.

Magnets

The SNR scales supra linearly with B_0 (13) and this is one of the major driving forces behind the trend to increase field strength. Superconducting magnets were an essential innovation on the road towards this goal. They are more stable against field drifts, but were technologically more demanding, requiring superconducting wire maintained at liquid helium temperature by a combination of electromagnetics, vacuum physics and refrigeration technology. These initially bulky, very heavy,

claustrophobia-inducing magnets became within two decades very compact and patient-friendly, with wider bores and a more open design. The first clinical 1.5T machines (60 cm bore) were in use by the mid 1980s and became 'wide bore' (70 cm) in the early 2000s.

Modern magnets are self-shielded, to reduce the fringe field to ease siting. However, this further increases the gradient of the static magnetic field close to the magnet, which increases the safety risk when ferro-magnetic objects are brought close to the magnet, making defined safety procedures for staff and patients necessary to reduce risk of injury. Magnets, furthermore, became significantly lighter, so that siting, even in the upper floors of hospitals is often no longer an issue. Although the external appearance of magnets has not changed very much, inside they are continuously being improved. Recently, 'cryo-free' magnet technology became available, allowing magnets with less than 10 litres liquid helium (a huge reduction from the previous value of about 1000 litres). This lowers costs in the unlikely case of a quench and further eases siting constraints because the quench line will soon be obsolete.

Meanwhile researchers are considering exploring the real human high-field limits with field strengths up to 14T currently being planned. Such systems are at present completely beyond clinical applicability and will probably remain forever in the research realm, because of their extremely high price, limited magnet production capacity and complex operation, including the management of unwanted physiological side effects. However, there is also a thriving research community operating at 7T and it will be interesting to see how this makes the transition to the clinic in the coming years, because some applications recently received approval from the US Food and Drug Administration (FDA). As anticipated in the early years of MRI,[6] RF wave propagation effects can seriously compromise high-field image quality and corresponding contrast. Parallel transmission,[14,15] schematically illustrated in Figure 1d, can mitigate those adverse effects, supporting RF shimming, which homogenises the RF transmit field, paving the way for high-quality 3T whole body-[16] or ultra-high-field head/torso imaging.

Despite this trend to pursue increased sensitivity by means of increasing the static magnetic field strength, there has recently been a small counter trend, to reconsider the use of lower field strengths.[17] One potential driver is the option to lower system costs, in some part also due to the lower interaction between patient and RF transmit fields, eliminating the need for parallel transmission technology, to mitigate wave propagation effects at high fields.[15–17] In addition, there is also the potential to reduce risk especially in interventional applications.[18]

Gradients

The room temperature bore of the magnet contains the gradient coil that performs the primary spatial encoding. The performance of the entire gradient system (c.f. Figure 1b) substantially influences the resulting image quality and has significantly improved with the introduction of self-shielded gradient coils[19–21] and the use of gradient pre-emphasis systems.[22] However, to speed-up data acquisition, higher sampling rates are necessary, which demands higher imaging gradient strength. The vendors answered this need by offering gradient systems with higher specifications (strength and slew rate), which often made a redesign of the gradient chain necessary, including the gradient coil interior,[23] the active cooling system and also the power amplifier operating principle, which moved to fully digitised switched mode devices. Today's gradient systems are high-tech/high-power electronic devices, running often at peak power levels close to a 1 MW.[24] This trend was compounded by the recent advent of wide bore systems, because the stored energy and thus the power requirements for a gradient coil increase with the fifth power of the diameter, and hence more than factor of 2 when the diameter just increases from 60 to 70cm.[25] Vendors have coped with these constraints by making compromises on gradient linearity, which have their main effect far from the iso-centre. However, the simple notion that higher gradient strengths offer higher speed is often not true anymore, because the maximum slew rate in imaging is often constrained by peripheral nerve stimulation (PNS) limits,[26] which get more critical in wide bore environments. Currently, there are some initial efforts to directly include PNS aspects as an additional constraint in the general coil design process[27] or to build dedicated high-end gradient coils restricting their effective fields only to small portions of the body like the head and thus minimising PNS.[28] It is interesting to note here that one of the main drivers of increased gradient strengths is the use of pulsed-field gradients to generate diffusion contrast. Higher gradients reduce the minimum echo time (TE) and thus reduce signal loss caused by T_2 decay.[29]

BASIC IMAGE ACQUISITION

Better gradients and faster spectrometers have enabled improved scanner performance, with shorter TRs, TEs and echo spacing and higher sampling rates—supporting modern acquisition techniques. This supported the development of accelerated multi-echo RF-refocused fast spin echo imaging,[30] which reduced the time associated with T_2 weighted acquisitions considerably. Similarly, for fast gradient echo imaging,[31] technological improvements have led to faster acquisitions of strongly T_1 weighted images.

Improved system performance[32] allowed the implementation of single shot Echo Planar Imaging[33] (EPI), for the first time breaking the dogma of sampling only in the presence of a constant read-out gradient. EPI has been the fastest imaging scheme available since the early 90s and is still the workhorse in many demanding applications: like fMRI, diffusion and perfusion imaging. This development represented in essence the first wave in terms of accelerating MRI. It was driven by the wish to shorten total examination time and to enhance patient throughput but also to reduce motion artefacts which increase with total scan time and or breath-hold duration. To further enhance the scope of these new sequences, numerous magnetisation preparation experiments[34,35] were designed to benefit from the new and more efficient gradient-echo and multi-spin-echo sampling schemes of the early 90s.

Figure 2. The evolution of MRI sampling schemes. Illustrated using 2D k-space sampling patterns. (a) Shows a radial scheme, the one MRI actually started with. (b) Cartesian sampling which took over due to its simplicity and robustness against hardware imperfections. (c) Spiral k-space sampling which maximises the sampling efficiency. (d) Hybrid radial–Cartesian sampling which is motion robust (each blade allows low resolution motion navigation). (e,f) Sub-sampling schemes for the dominant Cartesian schemes: (e) uniform sub-sampling as used in parallel imaging applications like SENSE and (f) variable density sub-sampling. A partially uniform version of (f) is used in GRAPPA while a more random version is used for compressed sensing.

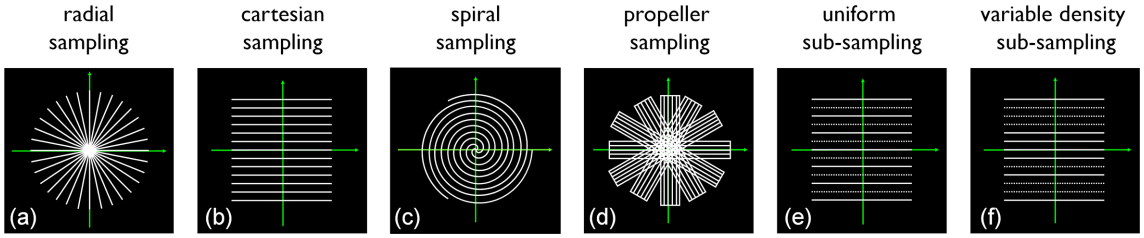

From the early 1990s, the improved main field homogeneity of magnets made possible the exploration of advanced alternative non-Cartesian k-space sampling schemes including spirals,[36,37] radial[38] and also hybrid schemes, mixing radial and Cartesian,[39] see Figure 2. These demanded non-uniform FFT or efficient regridding routines and often required dedicated field map field and concomitant field[40] gradient-based data corrections to cope with their increased off-resonance sensitivity.[41] Techniques like radial scanning gave an impetus to auto-correction[42] and auto-navigation,[43] which were developed to their full in the radial–Cartesian hybrid approach.[39]

CONTRAST

Many clinical applications were developed for almost all anatomies throughout the body. In the beginning, there was a focus on the brain and the central nervous system, followed by musculo-skeletal applications including extremities and joints. These organs were the easiest to image as they are relatively easy to immobilise for the duration of an MRI scan. As techniques for motion correction improved, body applications including spine, liver, lung, heart and pelvis became more common. Today there is almost no body part, which is not covered by MRI. Static diagnostic imaging was initially the primary focus, reflecting anatomy or different stages of pathology, but also dynamic/fluoroscopic or real-time imaging approaches[44,45] were developed to capture temporal changes such as heart motion or to utilise contrast media in the circulation to form MR angiograms.

The richness of the potential contrasts MRI can create is immense. Contrasts can be based on the Bloch equations, mainly driven by T_1 and T_2, the chemical shift effect, the chemical exchange of the water protons/magnetisation transfer, local magnetic susceptibility changes, but also on physiology-driven effects like flow, perfusion and diffusion. Thus, T_1 weighted and T_2 weighted imaging were performed using the fast gradient and turbo spin echo sequences. New sequences were designed like fluid-attenuated inversion recovery,[46] which can visualise abnormalities caused by subtle pathologies in the brain. Unlike in CT, where fat gives only a small signal, in MRI fat signal is often seen as a serious confounding factor. Therefore, fat suppression, performed by pre-saturation,[47] selective excitation, or by chemical shift encoding[48] has become a valuable tool to increase image contrast. However, the modern chemical shift encoding approaches[49] allow the separation of water and fat signals, leveraging also the information present in the fat to better understand obesity, the metabolic syndrome and to derive biomarkers in fat-related liver diseases.[50]

Another important contrast is diffusion, because it allows us to probe the tissue microstructure at a scale that is orders of magnitude below the actual image resolution.[51] The diffusion-weighted signal is read out preferably by single shot EPI[32] or TSE variants.[35] Diffusion helps to characterise tissue and tumours in type, state and grade non-invasively.[51] Applying different diffusion sensitisations (b-values) allows the calculation of an apparent diffusion coefficient (ADC) that can act as a bio-maker for stroke,[52] whereas probing diffusion in different spatial directions facilitates the estimation of the diffusion tensor that can map fibre orientations in the white matter of the brain[53] or in muscle. For brain imaging, the tensor formalism has largely been replaced by more sophisticated analysis techniques[54] that can interrogate multiple fibre orientations within a voxel. These require high angular resolution data acquisition, sometimes at multiple b-values. Knowledge of fibre distribution makes it possible to identify the major nerve bundles within the brain, which can be important for surgical planning, and to estimate the connectivity between grey matter regions, which is of great interest for neuroscientists.[54–56]Another extension of DWI is to examine the deviation from Gaussian diffusion, by using kurtosis imaging, which has proven to be very sensitive for tumour microstructure characterisation.[57]Other MR active nuclei (^{3}He, ^{13}C, ^{19}F, ^{129}Xe, etc.) can also be imaged giving access to new contrasts. If those nuclei have no or neglectable natural background signal in the body, they can be used as tracers, measuring MR properties of the compounds they label. This is a research branch on its own within MR which has already shown clinically relevant applications in lung imaging.[58]To illustrate the large range of contrasts accessible with MRI, some examples are given in Figure 3.

Around the turn of the millennium, the Radiological Society of North America (RSNA) declared the goal of transforming many imaging modalities, including MRI, into quantitative ones. Numbers were getting important! Numbers that can help to identify pathology and to quantify its state and extent and which can act as reliable biomarkers.[59] Numbers that can further help to bridge the gap between the contrasts of different

Figure 3. Selected MR contrasts and different anatomies for illustration. In the top row, different brain images are shown among them are T_1–T_2 weighted images, a fluid-attenuated inversion recovery (FLAIR), an MR angiogram, an inversion recovery (IR) image, a single shot diffusion scan (spiral, b = 1000 s/mm^2) and a fractional anisotropy (FA) map showing fibre anisotropy. The middle row shows a reformatted coronary angiogram, an amide proton transfer (APT) map in a tumour patient, two Dixon images (water only, water-fat in-phase), a diffusion-weighted whole-body image with background body signal suppression (DWIBS), a column of three single diffusion images (b-values 0, 100, 1000 s/mm^2) and a spine T_2 weighted image. In the bottom row, a flow-resolved cardiac image, a cardiac T_1 map to judge contrast media uptake quantitatively and two further Dixon images (water-fat out-phase, fat only) are shown.

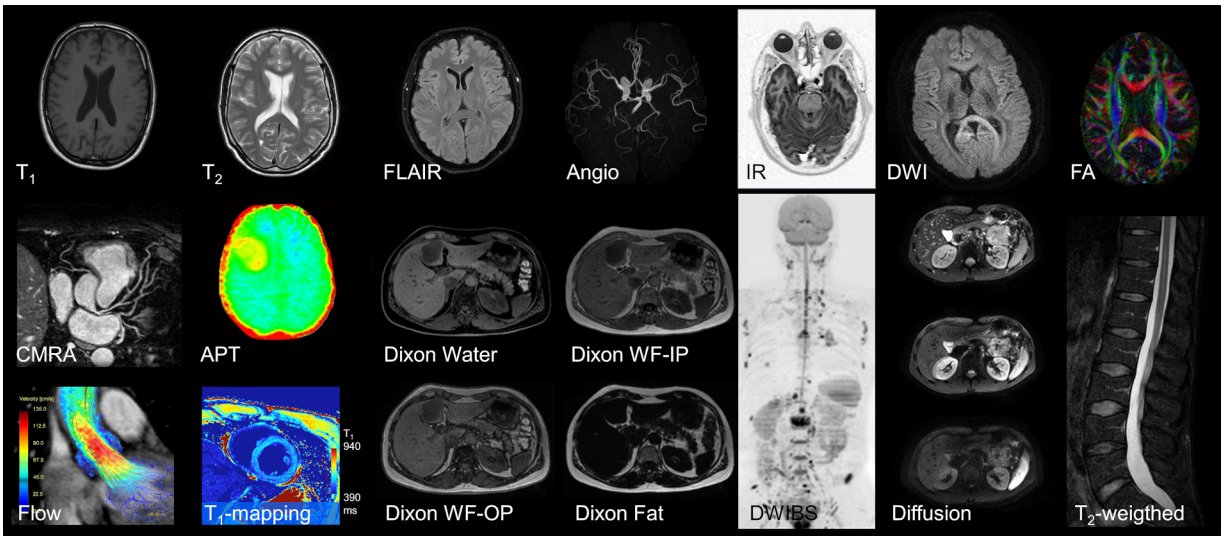

MR sequences, different field strengths and between the images of different vendors when using the same nominal acquisition technique. Numbers that can also help to assess potential therapy success or disease progression, like quantitative fat fraction mapping as a biomarker for hepatic steatosis[60] or amide protons targeting magnetisation transfer approaches, that can help to grade tumours.[61] Although initial studies, performed in the early days of MR,[62] revealed a large spread in the values of relaxation times in normal tissue, making reliable detection of pathology rather questionable, improved technology made it worthwhile reconsidering such concepts. This triggered the need for fast quantitative imaging to obtain values for MR measurable parameters like T_1, T_2, T_2^* and M_0. Next to accelerated versions of classical approaches for MR parameter-mapping, new techniques were developed very recently, among them MR finger printing[63] and MR stat.[64] To efficiently encode tissue properties, MR finger printing uses gradient-echo trains, preceded by spin inversion, with sequence parameters varying in time (such as TE, TR and the flip angle). The spatial information is encoded along those trains using heavily under sampled incoherent acquisition schemes, with spirals currently the preferred readout.[63] Using appropriate dictionaries, based on Bloch simulations, tissue characterisation and identification can be performed. This concept can be applied not only to T_1 and T_2 contrasts, but also to other applications like perfusion, water/fat imaging or other parameters which can be retrieved by an appropriate reconstruction.

Concepts of synthesising MR contrasts were revived[65] to synthesise via Bloch simulations' multiple contrasts with the hope to better visualise pathology.[66] However, it is not clear yet, how much these approaches will influence future clinical practice, and substantial further clinical work will be necessary to validate them and determine their ultimate value.

PARALLEL IMAGING

In the quest to further improve SNR either the available signal can be increased or the noise reduced. At clinical field strengths, the patient dominates the noise present in the receiver coil and thus in the receiver chain. Using smaller coils instead of a large body coil can help to reduce the detected noise level. The limited spatial coverage is then compensated by using an array of such small coils receiving the MR signal in parallel. This led to the birth of parallel imaging in the early 90s,[67] then understood simply as the use of multiple receiver coils independently contributing to the final image (c.f. Figure 1c). High-impedance pre-amplifier technology and geometric coil element overlapping approaches helped to reduce mutual coil coupling, considerably boosting SNR compared to conventional single body coil reception.[67–69] Manufacturers supported this trend rather quickly in two ways: first by offering MRI platforms that support many parallel receiving channels, and second by dedicated coil arrays for different anatomies, moving the fieldfrom 16 to 32 or even more channels for reception. Miniaturisation of necessary components, new coil designs and manufacturing principles helped to push these limits even further to massive parallel reception.[68,69] The use of up to 128 elements has been shown as a proof of principle, just to probe the real limits.[70,71] However, it has still to be proven whether this is the right balance between technical complexity, clinical usability, reliability/serviceability and affordability for MRI in the future. Apart from this simple number of elements- and channels-driven race, patient comfort is another important factor. Flexible[72] and surface adaptable, lightweight

coil arrays[73] have been proposed to support the examination of children[74] and very sick patients who are not able to stand bulky heavy coils. This is even today a field of active research and technological development.

Sense/GRAPPA

It took until the turn of the millennium before the hardware-dominated parallel imaging concept really revolutionised the entire MR acquisition methodology. This development represented in essence the second wave in terms of accelerating MRI, leading also to a new interpretation of the term parallel imaging, which today mainly means accelerated acquisition. Making the individual coils smaller, makes the detectable MR signal also dependent on the actual coil element positions and shape which gives access to a new and alternative spatial encoding principle that is complementary to the classical Fourier encoding process hitherto used in MR. Sensitivity encoding[75–77] became a powerful additional spatial encoding engine which quickly found adoption in commercial platforms mainly because of its simplicity, beauty and general applicability to all MR contrasts. The SNR gained by parallel reception could immediately be traded into acquisition speed by performing appropriate (mostly uniform k-space) under-sampling and corresponding unfolding of the reconstructed images either in the spatial[76] or in the k-space[77] domain. This second scan acceleration methodology was applicable to both MRI and MR spectroscopic imaging.[78]

Due to the simplicity of the phase encoding concept used in spin warp imaging, acceleration could be applied in one, two and more dimensions (spatial-, temporal-, parameter-encoded dimensions) immediately. However, successful image reconstruction relies on sufficient differentiation in the sensitivity profiles of the individual receiver coils, which can make the reconstruction ill-posed particularly at the centre of the object where receiver coil sensitivity is at its lowest, and the differential sensitivity between individual coils at its weakest. This led to the invaluable G-factor concept[76] that gives a measure for the conditioning of the parallel imaging reconstruction, which should be kept close to unity for satisfactory imaged quality. Coil compression concepts[79] can speed-up reconstruction, which is especially important in non-uniform sampling schemes.[80] G-factor noise propagation in the reconstruction process was reduced by smart and dedicated k-space sub-sampling schemes, which enabled better control of the aliasing in parallel imaging[81,82] and appropriate regularisation[83] in the reconstruction.

Recently the use of additional encoding gradients, applied simultaneously with the Cartesian read-out gradients, was proposed to enhance the controlled aliasing. This approach allows for an even better conditioning of the parallel imaging reconstruction,[84] bridging the conceptual gap to the sensitivity encoded accelerated non-Cartesian sampling world.[80]

However, apart from acceleration, the sensitivity encoding concept gave also new freedom for acoustic noise reduction by reducing the amount of gradient switching.[85] This burden for the patient can be lowered, while keeping the scanning time unaltered.

Multi-band/Simultaneous Multi-Slice

Parallel imaging can also be applied along the slice selection direction in multi-slice applications.[86] By taking advantage from the 3D variation in coil sensitivities, the signals of simultaneously excited multiple slices can be disentangled by parallel imaging. However, it took almost a full decade before robust sub-sampling schemes[87] and widespread availability of multi-channel receive coils helped to better pre-condition the unfolding problem, finally facilitating simultaneous multi-band imaging which shows the benefit of almost no SNR penalty due to the low G-factor burden. To mitigate potential RF peak power and specific absorption rate-related issues, optimal phase design for the multi-band RF pulses involved has been proposed.[88] The multi-band option nicely bridged the gap between multi-slice and 3D acquisitions, because clinically there are many sampling schemes, which are often not performed in 3D, for instance fMRI or single shot diffusion EPI, and are not appreciably accelerated by standard parallel imaging, as they have to be performed at a fixed TE.[89]

Model-based reconstruction

Parallel imaging increased the quantity of MR data substantially and turned MR reconstruction into an over determined problem, that is, there are simply more measured data points than pixels to be finally reconstructed. The redundancy in the multi-channel data was primarily used to boost SNR, but offers additional options to enforce data consistency, ruling out potential outliers or corrupted data[90,91] to make the best out of the available data and finally improve the overall image quality including the SNR. These model-based reconstruction approaches[92] still form an active field of research and are supported by recent advances in linear and non-linear numerical solvers. Depending on the signal model assumed for the image formation process and the cost function, relevant model parameters like coil sensitivities[93] can be estimated or updated along with the final image. This could help to mitigate inconsistencies and resulting image quality problems when actual and pre-measured coil sensitivities differ due to patient motion. Other confounding scanning conditions can also be modelled, such as for instance gross motion,[94] physiology-induced phase changes[95] or motion artefacts in segmented diffusion acquisition[96] or B_0 fluctuations in gradient-echo imaging.[97]

Not all of these proposed methods have yet found a place in daily clinical scanning practice, because they also change the image reconstruction process significantly, from simple pipelines into iterative loops which are often rather time consuming and could benefit from further numerical and/or computer hardware speed-ups.

COMPRESSED SENSING

The sampling community had not yet assimilated all aspects of accelerated parallel imaging, when the next wave of scan acceleration arrived. Previously MR sampling schemes were based on the Nyquist sampling theorem. However, the robustness of radial imaging against under-sampling, seen already in the early days, made it plausible that alternatives might be viable. Compressed sensing (CS)[98] is a new sampling paradigm, proven

Figure 4. Comparison SENSE and compressed SENSE. Slices of a retrospectively under-sampled 3D T_2 weighted TSE data set reconstructed with different acceleration factors and sampling methods (SENSE/Compressed SENSE) using a 15-element head coil (voxel 1.0×1.0×1.2 mm^3, 3T). Formally the 4×4 accelerated case is already under-determined. The advantage of variable density sampling and compressed sensing reconstruction over SENSE is obvious. Please note that there is no claim that the 4×4 variable density CS image is of clinical diagnostic value.

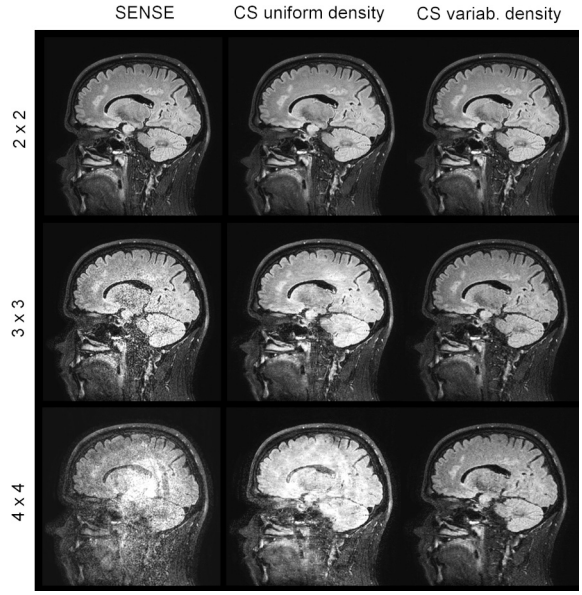

Figure 5. Accelerating MRI using an iterative AI/deep learning-based compressed-sensing approach. Clinical knee data (arXiv 1811.08839, 2018) measured with a 15-channel knee coil at two different contrasts were retrospectively variable density under-sampled and reconstructed. (a,d) Using zero filling, Fourier transform and coil image combination, (b,e) by an iterative AI-CS approach, whereas (c,f) show the ground truth for comparison. (top row: proton density, acceleration factor: 7.9, bottom row: T_2 weighted data, acceleration factor: 9.7). A quite high correspondence between the AI-driven reconstruction and the ground truth can be found and the ability to gently de-noise can be appreciated too. The reconstructions shown in the middle are from the winner of the fMRI reconstruction challenge multi-coil 8x and co-winner of the multi-coil 4x; courtesy Nicola Pezzotti, et al. 'Philips & LUMC' team (arXiv 1912.12259, 2019).

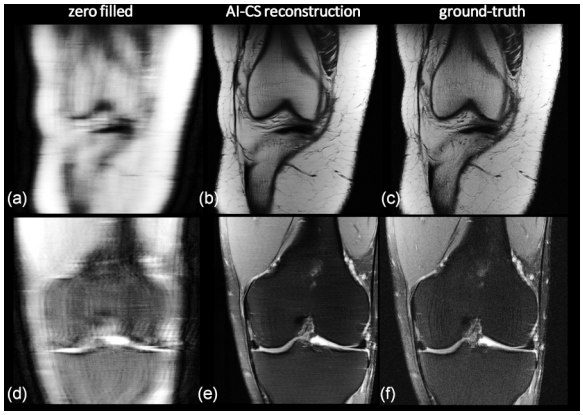

by mathematicians, demonstrating that images can correctly be reconstructed from even less data than usually sampled. To explore CS, the underlying signal distribution must be sparse, what seems to be the case in many MR applications, an incoherent sampling scheme has to be used and a sparsity enforcing (iterative) reconstruction has to be employed to reduce the pseudo-noise introduced by the unconventional sampling process, which can be realised using a dedicated cost function model-based reconstruction.[92] It turned out that CS enables additional acceleration on top of parallel imaging by roughly a factor two and potentially even more, when more sparse encoding dimensions are involved.[99,100] This substantial extra acceleration, the compatibility to parallel imaging (c.f. Figure 4) and with many current clinical protocols, made CS very attractive so that it rapidly found FDA approval[101] and early adoption in clinical practice.

DEEP LEARNING AND ARTIFICIAL INTELLIGENCE

Since about 2015 another trend emerged when it was shown that artificial intelligence (AI) can outperform humans in selected tasks.[102] So, registration and segmentation, typical classical image processing tasks have been shown to be better performed by AI.[102] Many typical MR artefacts, with the motion-induced ones being the most critical, can be learned, identified and removed from MRI images.[103,104] In addition to those post-processing applications, AI approaches have already been applied to reconstruct the image directly from under-sampled k-space data.[105] One can argue whether it is useful to learn the FFT for which we have already very efficient algorithms, or whether the huge memory needed to form the fully connected layers that are necessary for that purpose are really justified, but at least it shows the huge potential of AI, even when it is just as an element in our current model-based reconstructions.[106,107] Iterative algorithms can also be seen as a recurrent neural network consisting of different layers with simple operations in between optimised in a data-driven/learning-based fashion.[108] This is the current situation, at a cusp between model—driven to data—driven approaches which can be expected to nicely complement each other in the future (Figure 5).

Networks can learn the optimal sparsifying transform and the corresponding regularisation parameters, often critical in many modern model-based reconstructions[109] and can also be helpful in final image de-noising.[110] Furthermore, they have another benefit when the appropriately trained reconstruction model is in place, the actual computation for reconstructing a new data set can be extremely fast.

However, despite the improvements achievable with machine learning compared to classical or iterative approaches, there is a concern that neural networks have a black-box nature and that there is no closed theory foundation about them available.[106] However, there is no doubt, deep learning in medical image formation, data analysis and augmented image interpretation and diagnosis is here to stay. As a community we need more experience in the machine learning area just to determine

which problems can be completely solved using deep learning techniques, which are better handled by a combination of deep learning with other techniques, or for which no deep learning component is needed at all.[102]

WORKFLOW

One further important aspect of operating an MRI system today is workflow to guarantee highest diagnostic value, optimal scan efficacy, and best patient comfort and safety. In many aspects here, the MR radiographer is key. Back in the early days, technicians were MR experts, but today they have to have other skills too. They manage multiple tasks, sometimes multiple systems, often multiple modalities, and most importantly, they often handle many different patients simultaneously. Today's radiographers have to fix scheduling issues, instruct and prepare the patient, ensuring that the patient is metal-free (especially ferro magnetic), add physiology sensors, place coils properly, ensure safe patient positioning in the magnet and finally run the different clinical scans, not only maximising image quality but also making decisions which potential scan should be added or skipped to appropriately support final diagnosis.

This will become an area of substantial work in the future, and it will lead to concepts of complexity-reduced and auto-driven scanners, with real-time auto-triaging capabilities, freeing the operator from boring standard work to better deal with the patient, increasing patient-comfort and diagnostic confidence.

In that respect, we can also expect changes in the way MRI will be used in the future. Currently MR often comes at the end of the diagnostic chain with the aim to finalise an often unclear diagnosis. This results in long total examination times adding more scans to get a comprehensive radiological view of the patients' problem. However, this can change in the future, because recently also 5 min comprehensive exams arrived on the radiologist's wish list, next to the more extensive traditional scanning protocols. These fast exams can further reduce table times, paving the way for applying MR as a test, and can further change the way we perform MRI.

CONCLUDING REMARKS

Looking back on those 50 years, MRI has already come a long way, and there is still lots of room for considerable development in the future. With the ability to probe the local tissue environment, via multiple MR contrasts, and with the development of fast and motion-still sequences, we went as a community a long way towards improving the diagnostic image quality and value of MRI. We improved acquisition speed with strong gradients, parallel imaging and compressed sensing and in the future advanced model-driven and AI supported reconstruction algorithms will allow us to obtain more reliable and better diagnostic information, increasing diagnostic confidence and offering a convenient and highly patient-oriented service.

Again, it needs a single human to have a great idea, but a whole community of medical physicists, MR-physicists, engineers, radiographers, physicians and all patients to make it really fly!

ACKNOWLEDGMENT

Many thanks to Dr Christian Stehning and Dr Hendrik Kooijman who helped to compile Figure 3.

FUNDING

Peter Börnert, David G Norris: no relevant grants have to be mentioned.

REFERENCES

1. Holtzmann Kevles B, Holtzmann Kevles B. *Naked to the bone: medical imaging in the twentieth century*: Rutgers University Press; 1998. pp. 978–201328332.
2. Lauterbur PC. Image formation by induced local interactions: examples employing nuclear magnetic resonance. *Nature* 1973; **242**: 190–1. doi: https://doi.org/10.1038/242190a0
3. Damadian R. Tumor detection by nuclear magnetic resonance. *Science* 1971; **171**: 1151–3. doi: https://doi.org/10.1126/science.171.3976.1151
4. Edelstein WA, Hutchison JMS, Johnson G, Redpath T. Spin warp NMR imaging and applications to human whole-body imaging. *Phys Med Biol* 1980; **25**: 751–6. doi: https://doi.org/10.1088/0031-9155/25/4/017
5. Crooks L, Arakawa M, Hoenninger J, Watts J, McRee R, Kaufman L, et al. Nuclear magnetic resonance whole-body imager operating at 3.5 KGauss. *Radiology* 1982; **143**: 169–74. doi: https://doi.org/10.1148/radiology.143.1.7063722
6. Mansfield P, Morris PG. Advances in Magnetic Resonance. In: *NMR Imaging in Biomedicine*. **Suppl. 2**. *New York*: Academic Press; 1982. pp. 187.
7. Twieg DB. The *k* -trajectory formulation of the NMR imaging process with applications in analysis and synthesis of imaging methods. *Med Phys* 1983; **10**: 610–21. doi: https://doi.org/10.1118/1.595331
8. Ljunggren S. A simple graphical representation of fourier-based imaging methods. *Journal of Magnetic Resonance* 1983; **54**: 338–43. doi: https://doi.org/%2010.1016/0022-2364(83)90060-4
9. Ehman EC, Johnson GB, Villanueva-Meyer JE, Cha S, Leynes AP, Larson PEZ, et al. Pet/Mri: where might it replace PET/CT? *J. Magn. Reson. Imaging* 2017; **46**: 1247–62. doi: https://doi.org/10.1002/jmri.25711
10. Hall WA, Paulson ES, van der Heide UA. Atlantic Consortium and the ViewRay C2T2 research Consortium.cThe transformation of radiation oncology using real-time magnetic resonance guidance: a review. *Eur J Cancer* 2019; **122**: 42–52.
11. Mansfield P, Maudsley AA. Planar spin imaging by NMR. *J. Phys. C: Solid State Phys.* 1976; **9**: L409–12. doi: https://doi.org/10.1088/0022-3719/9/15/004
12. Hutchinson JMS, Sutherland RJ, Mallard JR. Nmr imaging: image recovery under magnetic fields with large non-uniformities. *J. Phys. E: Sci. Instrum.* 1978; **11**: 217–22. doi: https://doi.org/10.1088/0022-3735/11/3/012
13. Redpath TW. Signal-To-Noise ratio in MRI. *Br J Radiol* 1998; **71**: 704–7. doi: https://doi.org/10.1259/bjr.71.847.9771379

14. Katscher U, Börnert P, Leussler C, van den Brink JS. Transmit sense. *Magn. Reson. Med.* 2003; ; **49**: 144–50Jan. doi: https://doi.org/10.1002/mrm.10353
15. Zhu Y. Parallel excitation with an array of transmit coils. *Magn. Reson. Med.* 2004; **51**: 775–84. doi: https://doi.org/10.1002/mrm.20011
16. Nelles M, König RS, Gieseke J, Guerand-van Battum MM, Kukuk GM, Schild HH, et al. Dual-source parallel rf transmission for clinical MR imaging of the spine at 3.0 T: Intraindividual comparison with conventional single-source transmission. *Radiology* 2010; **257**: 743–53. doi: https://doi.org/10.1148/radiol.10092146
17. Marques JP, Simonis FFJ, Webb AG. Low-field MRI: an Mr physics perspective. *J. Magn. Reson. Imaging* 2019; **49**: 1528–42. doi: https://doi.org/10.1002/jmri.26637
18. Campbell-Washburn AE, Ramasawmy R, Restivo MC, Bhattacharya I, Basar B, Herzka DA, et al. Opportunities in interventional and diagnostic imaging by using high-performance Low-Field-Strength MRI. *Radiology* 2019; **293**: 384–93. doi: https://doi.org/10.1148/radiol.2019190452
19. Roemer PB, Hickey JS. Self-shielded gradient coils for nuclear magnetic resonance imaging. *European Patent Application* 1986; **87**: 198.
20. Turner R. A target field approach to optimal coil design. *J. Phys. D: Appl. Phys.* 1986; **19**: L147–51. doi: https://doi.org/10.1088/0022-3727/19/8/001
21. Mansfield P, Chapman B. Active magnetic screening of gradient coils in NMR imaging. *Journal of Magnetic Resonance* 1986; **66**: 573–6. doi: https://doi.org/10.1016/0022-2364(86)90205-2
22. Van Vaals JJ, Bergman AH. Optimization of eddy-current compensation. *Journal of Magnetic Resonance* 1990; **90**: 52–70. doi: https://doi.org/10.1016/0022-2364(90)90365-G
23. Turner R. Gradient coil design: a review of methods. *Magn Reson Imaging* 1993; **11**: 903–20. doi: https://doi.org/10.1016/0730-725X(93)90209-V
24. Hidalgo-Tobon SS. Theory of gradient coil design methods for magnetic resonance imaging. *Concepts in Magnetic Resonance Part A* 2010; **36A**: 223–42. doi: https://doi.org/10.1002/cmr.a.20163
25. Golay MJE. Field Homogenizing coils for nuclear spin resonance instrumentation. *Review of Scientific Instruments* 1958; **29**: 313–5. doi: https://doi.org/10.1063/1.1716184
26. Davids M, Guérin B, Malzacher M, Schad LR, Wald LL. Predicting Magnetostimulation thresholds in the peripheral nervous system using realistic body models. *Sci Rep* 2017; **7**: 5316. doi: https://doi.org/10.1038/s41598-017-05493-9
27. Davids M, Guérin B, vom Endt A, Schad LR, Wald LL. Prediction of peripheral nerve stimulation thresholds of MRI gradient coils using coupled electromagnetic and neurodynamic simulations. *Magn. Reson. Med* 2019; **81**: 686–701. doi: https://doi.org/10.1002/mrm.27382
28. Weiger M, Overweg J, Rösler MB, Froidevaux R, Hennel F, Wilm BJ, et al. A high-performance gradient insert for rapid and short-T_2 imaging at full duty cycle. *Magn. Reson. Med* 2018; **79**: 3256–66. doi: https://doi.org/10.1002/mrm.26954
29. Burdette JH, Elster AD, Ricci PE. Acute cerebral infarction: quantification of spin-density and T2 shine-through phenomena on diffusion-weighted Mr images. *Radiology* 1999; **212**: 333–9. doi: https://doi.org/10.1148/radiology.212.2.r99au36333
30. Hennig J, Nauerth A, Friedburg H. Rare imaging: a fast imaging method for clinical Mr. *Magn Reson Med* 1986; **3**: 823–33. doi: https://doi.org/10.1002/mrm.1910030602
31. Haase A, Frahm J, Matthaei D, Hanicke W, Merboldt K-D. Flash imaging. rapid NMR imaging using low flip-angle pulses. *Journal of Magnetic Resonance* 1986; **67**: 258–66. doi: https://doi.org/10.1016/0022-2364(86)90433-6
32. Rzedzian R, Doyle M, Mansfield P, Chapman B, Guilfoyle C, Coupland P, et al. *Lancet* 1983; **2**: 1281–2.
33. Mansfield P. Multi-planar image formation using NMR spin echoes. *J. Phys. C: Solid State Phys.* 1977; **10**: L55–8. doi: https://doi.org/10.1088/0022-3719/10/3/004
34. Haase A, Snapshot FLASH MRI. Applications to T1, T2, and chemical-shift imaging. *MagnReson Med* 1990; **13**: 77–89. doi: https://doi.org/10.1002/mrm.1910130109
35. Norris DG, Börnert P, Reese T, Leibfritz D. On the application of ultra-fast rare experiments. *Magn. Reson. Med.* 1992; **27**: 142–64. doi: https://doi.org/10.1002/mrm.1910270114
36. Ahn CB, Kim JH, Cho ZH. High-Speed Spiral-Scan echo planar NMR Imaging-I. *IEEE Trans Med Imaging* 1986; **5**: 2–7. doi: https://doi.org/10.1109/TMI.1986.4307732
37. Meyer CH, Hu BS, Nishimura DG, Macovski A. Fast spiral coronary artery imaging. *Magn. Reson. Med.* 1992; **28**: 202–13. doi: https://doi.org/10.1002/mrm.1910280204
38. Glover GH, Pauly JM. Projection reconstruction techniques for reduction of motion effects in MRI. *Magn. Reson. Med.* 1992; **28**: 275–89. doi: https://doi.org/10.1002/mrm.1910280209
39. Pipe JG. Motion correction with propeller MRI: application to head motion and free-breathing cardiac imaging. *Magn. Reson. Med.* 1999; **42**: 963–9. doi: https://doi.org/10.1002/(SICI)1522-2594(199911)42:5<963::AID-MRM17>3.0.CO;2-L
40. Norris DG, Hutchison JMS. Concomitant magnetic field gradients and their effects on imaging at low magnetic field strengths. *Magn Reson Imaging* 1990; **8**: 33–7. doi: https://doi.org/10.1016/0730-725X(90)90209-K
41. Börnert P, Schomberg H, Aldefeld B, Groen J. Improvements in spiral MR imaging. *MAGMA* 1999; **9**(1-2): 29–41. doi: https://doi.org/10.1007/BF02634590
42. Rasche V, Holz D, Proksa R. Mr fluoroscopy using projection reconstruction multi-gradient-echo (prMGE) MRI. *Magn. Reson. Med.* 1999; **42**: 324–34. doi: https://doi.org/10.1002/(SICI)1522-2594(199908)42:2<324::AID-MRM15>3.0.CO;2-R
43. Schäffter T, Rasche V, Carlsen IC. Motion compensated projection reconstruction. *Magn Reson Med* 1999; **41**: 954–63. doi: https://doi.org/10.1002/(SICI)1522-2594(199905)41:5<954::AID-MRM15>3.0.CO;2-J
44. Riederer SJ, Tasciyan T, Farzaneh F, Lee JN, Wright RC, Herfkens RJ. Mr fluoroscopy: technical feasibility. *Magn. Reson. Med.* 1988; **8**: 1–15. doi: https://doi.org/10.1002/mrm.1910080102
45. Pearlman JD, Edelman RR. Ultrafast magnetic resonance imaging. segmented turboflash, echo-planar, and real-time nuclear magnetic resonance. *Radiol Clin North Am* 1994; **32**: 593–612.
46. Hajnal JV, Bryant DJ, Kasuboski L, Pattany PM, Coene BD, Lewis PD, et al. Use of fluid attenuated inversion recovery (FLAIR) pulse sequences in MRI of the brain. *J Comput Assist Tomogr* 1992; **16**: 841–4. Nov-Dec;. doi: https://doi.org/10.1097/00004728-199211000-00001
47. Haase A, Frahm J, Hänicke W, Matthaei D. ^{1}H NMR chemical shift selective (CHESS) imaging. *Phys Med Biol* 1985; **30**: 341–4. doi: https://doi.org/10.1088/0031-9155/30/4/008
48. Dixon WT. Simple proton spectroscopic imaging. *Radiology* 1984; **153**: 189–94. doi: https://doi.org/10.1148/radiology.153.1.6089263
49. Reeder SB, Wen Z, Yu H, Pineda AR, Gold GE, Markl M, et al. Multicoil Dixon chemical species separation with an iterative least-squares estimation method. *Magn. Reson. Med.* 2004; **51**: 35–45. doi: https://doi.org/10.1002/mrm.10675

50. Hu HH, Börnert P, Hernando D, Kellman P, Ma J, Reeder S, et al. ISMRM workshop on fat-water separation: insights, applications and progress in MRI. *Magn Reson Med* 2012; **68**: 378–88. doi: https://doi.org/10.1002/mrm.24369
51. Le Bihan D, Breton E, Lallemand D, Grenier P, Cabanis E, Laval-Jeantet M. Mr imaging of intravoxel incoherent motions: application to diffusion and perfusion in neurologic disorders. *Radiology* 1986; **161**: 401–7. doi: https://doi.org/10.1148/radiology.161.2.3763909
52. Moseley ME, Butts K, Yenari MA, Marks M, Crespigny AD. Clinical aspects of DWI. *NMR Biomed* 1995; **8**(7-8): 387–96. Nov-Dec. doi: https://doi.org/10.1002/nbm.1940080712
53. Mori S, Kaufmann WE, Davatzikos C, Stieltjes B, Amodei L, Fredericksen K, et al. Imaging cortical association tracts in the human brain using diffusion-tensor-based axonal tracking. *Magn. Reson. Med.* 2002; **47**: 215–23. doi: https://doi.org/10.1002/mrm.10074
54. Jbabdi S, Johansen-Berg H. Tractography: where do we go from here? *Brain Connect* 2011; **1**: 169–83. doi: https://doi.org/10.1089/brain.2011.0033
55. Jeurissen B, Descoteaux M, Mori S, Leemans A. Diffusion MRI fiber tractography of the brain. *NMR Biomed* 2019; **32**: e3785. doi: https://doi.org/10.1002/nbm.3785
56. Minati L, Węglarz WP. Physical foundations, models, and methods of diffusion magnetic resonance imaging of the brain: a review. *Concepts in Magnetic Resonance Part A* 2007; **30A**: 278–30737. doi: https://doi.org/10.1002/cmr.a.20094
57. Szczepankiewicz F, van Westen D, Englund E, Westin C-F, Ståhlberg F, Lätt J, et al. The link between diffusion MRI and tumor heterogeneity: mapping cell eccentricity and density by diffusional variance decomposition (divide. *Neuroimage* 2016; **142**: 522–32. doi: https://doi.org/10.1016/j.neuroimage.2016.07.038
58. Kern AL, Vogel-Claussen J. Hyperpolarized gas MRI in pulmonology. *Br J Radiol* 2018; **53**: 20170647. doi: https://doi.org/10.1259/bjr.20170647
59. https://www.rsna.org/en/research/quantitative-imaging-biomarkers-alliance
60. Reeder SB, Hu HH, Sirlin CB. Proton density fat-fraction: a standardized mr-based biomarker of tissue fat concentration. *J. Magn. Reson. Imaging* 2012; **36**: 1011–4. doi: https://doi.org/10.1002/jmri.23741
61. Togao O, Yoshiura T, Keupp J, Hiwatashi A, Yamashita K, Kikuchi K, et al. Amide proton transfer imaging of adult diffuse gliomas: correlation with histopathological grades. *Neuro Oncol* 2014; **16**: 441–8. doi: https://doi.org/10.1093/neuonc/not158
62. Bottomley PA, Hardy CJ, Argersinger RE, Allen-Moore G. A review of 1H nuclear magnetic resonance relaxation in pathology: are T1 and T2 diagnostic? *Med Phys* 1987; **14**: 1–37. doi: https://doi.org/10.1118/1.596111
63. Ma D, Gulani V, Seiberlich N, Liu K, Sunshine JL, Duerk JL, et al. Magnetic resonance fingerprinting. *Nature* 2013; ; **495**: 187–9214. doi: https://doi.org/10.1038/nature11971
64. Sbrizzi A, Heide Ovander, Cloos M, Toorn Avander, Hoogduin H, Luijten PR, et al. Fast quantitative MRI as a nonlinear tomography problem. *Magn Reson Imaging* 2018; **46**: 56–63. doi: https://doi.org/10.1016/j.mri.2017.10.015
65. Bobman SA, Riederer SJ, Lee JN, Suddarth SA, Wang HZ, Drayer BP, et al. Cerebral magnetic resonance image synthesis. *AJNR Am J Neuroradiol* 1985; **6**: 265–9. Mar-Apr.
66. Andica C, Hagiwara A, Hori M, Kamagata K, Koshino S, Maekawa T, et al. Review of synthetic MRI in pediatric brains: basic principle of Mr quantification, its features, clinical applications, and limitations. *Journal of Neuroradiology* 2019; **46**: 268–75. doi: https://doi.org/10.1016/j.neurad.2019.02.005
67. Roemer PB, Edelstein WA, Hayes CE, Souza SP, Mueller OM. The NMR phased array. *Magn Reson Med* 1990; **16**: 192–225. doi: https://doi.org/10.1002/mrm.1910160203
68. Wiesinger F, Boesiger P, Pruessmann KP. Electrodynamics and ultimate SNR in parallel MR imaging. *Magn. Reson. Med.* 2004; **52**: 376–90. doi: https://doi.org/10.1002/mrm.20183
69. Keil B, Wald LL. Massively parallel MRI detector arrays. *Journal of Magnetic Resonance* 2013; **229**: 75–89. doi: https://doi.org/10.1016/j.jmr.2013.02.001
70. Schmitt M, Potthast A, Sosnovik DE, Polimeni JR, Wiggins GC, Triantafyllou C, et al. A 128-channel receive-only cardiac coil for highly accelerated cardiac MRI at 3 tesla. *Magn. Reson. Med.* 2008; **59**: 1431–9. doi: https://doi.org/10.1002/mrm.21598
71. Hardy CJ, Giaquinto RO, Piel JE, Rohling AAS KW, Marinelli L, Blezek DJ, et al. 128-channel body MRI with a flexible high-density receiver-coil array. *J. Magn. Reson. Imaging* 2008; **28**: 1219–25. doi: https://doi.org/10.1002/jmri.21463
72. Nordmeyer-Massner JA, De Zanche N, Pruessmann KP. Stretchable coil arrays: application to knee imaging under varying flexion angles. *Magn. Reson. Med.* 2012; **67**: 872–9. doi: https://doi.org/10.1002/mrm.23240
73. McGee KP, Stormont RS, Lindsay SA, Taracila V, Savitskij D, Robb F, et al. Characterization and evaluation of a flexible MRI receive coil array for radiation therapy Mr treatment planning using highly decoupled rf circuits. *Phys. Med. Biol.* 2018; **63**: 08NT0208NT02. doi: https://doi.org/10.1088/1361-6560/aab691
74. Zhang T, Grafendorfer T, Cheng JY, Ning P, Rainey B, Giancola M, et al. A semiflexible 64-channel receive-only phased array for pediatric body MRI at 3T. *Magn. Reson. Med.* 2016; **76**: 1015–21. doi: https://doi.org/10.1002/mrm.25999
75. Sodickson DK, Manning WJ. Simultaneous acquisition of spatial harmonics (SMASH): fast imaging with radiofrequency coil arrays. *Magn. Reson. Med.* 1997; **38**: 591–603. doi: https://doi.org/10.1002/mrm.1910380414
76. Pruessmann KP, Weiger M, Scheidegger MB, Boesiger P. Sense: sensitivity encoding for fast MRI. *Magn. Reson. Med.* 1999; **42**: 952–62. doi: https://doi.org/10.1002/(SICI)1522-2594(199911)42:5<952::AID-MRM16>3.0.CO;2-S
77. Griswold MA, Jakob PM, Heidemann RM, Nittka M, Jellus V, Wang J, et al. Generalized autocalibrating partially parallel acquisitions (grappa. *Magn. Reson. Med.* 2002; **47**: 1202–10. doi: https://doi.org/10.1002/mrm.10171
78. Dydak U, Weiger M, Pruessmann KP, Meier D, Boesiger P. Sensitivity-encoded spectroscopic imaging. *Magn. Reson. Med.* 2001; **46**: 713–22. doi: https://doi.org/10.1002/mrm.1250
79. Buehrer M, Pruessmann KP, Boesiger P, Kozerke S. Array compression for MRI with large coil arrays. *Magn. Reson. Med.* 2007; **57**: 1131–9. doi: https://doi.org/10.1002/mrm.21237
80. Pruessmann KP, Weiger M, Börnert P, Boesiger P. Advances in sensitivity encoding with arbitrary *k* -space trajectories. *Magn. Reson. Med.* 2001; **46**: 638–51. doi: https://doi.org/10.1002/mrm.1241
81. Breuer FA, Blaimer M, Mueller MF, Seiberlich N, Heidemann RM, Griswold MA, et al. Controlled aliasing in volumetric parallel imaging (2D CAIPIRINHA. *Magn. Reson. Med.* 2006; **55**: 549–56. doi: https://doi.org/10.1002/mrm.20787
82. Tsao J, Kozerke S, Boesiger P, Pruessmann KP. Optimizing spatiotemporal sampling fork-t blast andk-t sense: application to high-resolution real-time cardiac steady-state free precession. *Magn. Reson. Med.* 2005; **53**: 1372–82. doi: https://doi.org/10.1002/mrm.20483

83. Lin F-H, Kwong KK, Belliveau JW, Wald LL. Parallel imaging reconstruction using automatic regularization. *Magn. Reson. Med.* 2004; **51**: 559–67. doi: https://doi.org/10.1002/mrm.10718
84. Bilgic B, Gagoski BA, Cauley SF, Fan AP, Polimeni JR, Grant PE, et al. Wave-CAIPI for highly accelerated 3D imaging. *Magn. Reson. Med.* 2015; **73**: 2152–62. doi: https://doi.org/10.1002/mrm.25347
85. de Zwart JA, van Gelderen P, Kellman P, Duyn JH. Reduction of gradient acoustic noise in MRI using SENSE-EPI. *Neuroimage* 2002; **16**: 1151–5. doi: https://doi.org/10.1006/nimg.2002.1119
86. Larkman DJ, Hajnal JV, Herlihy AH, Coutts GA, Young IR, Ehnholm G. Use of multicoil arrays for separation of signal from multiple slices simultaneously excited. *J Magn Reson Imaging* 2001; **13**: 313–7. doi: https://doi.org/10.1002/1522-2586(200102)13:2<313::AID-JMRI1045>3.0.CO;2-W
87. Breuer FA, Blaimer M, Heidemann RM, Mueller MF, Griswold MA, Jakob PM. Controlled aliasing in parallel imaging results in higher acceleration (CAIPIRINHA) for multi-slice imaging. *Magn. Reson. Med.* 2005; **53**: 684–91. doi: https://doi.org/10.1002/mrm.20401
88. Hennig J. Chemical shift imaging with phase-encoding rf pulses. *Magn. Reson. Med.* 1992; **25**: 289–98. doi: https://doi.org/10.1002/mrm.1910250207
89. Moeller S, Yacoub E, Olman CA, Auerbach E, Strupp J, Harel N, et al. Multiband multislice GE-EPI at 7 Tesla, with 16-fold acceleration using partial parallel imaging with application to high spatial and temporal whole-brain fMRI. *Magn. Reson. Med.* 2010; **63**: 1144–5364. doi: https://doi.org/10.1002/mrm.22361
90. Bydder M, Atkinson D, Larkman DJ, Hill DLG, Hajnal JV. SMASH navigators. *Magn. Reson. Med.* 2003; ; **49**: 493–500Mar. doi: https://doi.org/10.1002/mrm.10388
91. Winkelmann R, Börnert P, Dössel O. Ghost artifact removal using a parallel imaging approach. *Magn. Reson. Med.* 2005; **54**: 1002–9. doi: https://doi.org/10.1002/mrm.20640
92. Fessler J. Model-Based image reconstruction for MRI. *IEEE Signal Process Mag* 2010; ; **27**: 81–91. doi: https://doi.org/10.1109/MSP.2010.936726
93. Ying L, Sheng J. Joint image reconstruction and sensitivity estimation in sense (JSENSE. *Magn. Reson. Med.* 2007; **57**: 1196–202. doi: https://doi.org/10.1002/mrm.21245
94. Odille F, Vuissoz P-A, Marie P-Y, Felblinger J. Generalized reconstruction by inversion of coupled systems (GRICS) applied to free-breathing MRI. *Magn. Reson. Med.* 2008; **60**: 146–57. doi: https://doi.org/10.1002/mrm.21623
95. Guo H, Ma X, Zhang Z, Zhang B, Yuan C, Huang F. POCS-enhanced inherent correction of motion-induced phase errors (POCS-ICE) for high-resolution multishot diffusion MRI. *Magn. Reson. Med.* 2016; **75**: 169–80. doi: https://doi.org/10.1002/mrm.25594
96. Steinhoff M, Nehrke K, Mertins A, Börnert P. Segmented diffusion imaging with iterative motion-corrected reconstruction (sediment) for brain echo-planar imaging. *NMR Biomed* 2019; **13**: e4185. doi: https://doi.org/10.1002/nbm.4185
97. Meineke J, Nielsen T. Data consistency-driven determination of B0-fluctuations in gradient-echo MRI. *Magn Reson Med* 2019; **81**: 3046–55. doi: https://doi.org/10.1002/mrm.27630
98. Lustig M, Donoho D, Pauly JM. Sparse MRI: the application of compressed sensing for rapid MR imaging. *Magn Reson Med* 2007; **58**: 1182–95. doi: https://doi.org/10.1002/mrm.21391
99. Murphy M, Alley M, Demmel J, Keutzer K, Vasanawala S, Lustig M. Fast ℓ_1-SPIRiT Compressed Sensing Parallel Imaging MRI: Scalable Parallel Implementation and Clinically Feasible Runtime. *IEEE Trans Med Imaging* 2012; **31**: 1250–62. doi: https://doi.org/10.1109/TMI.2012.2188039
100. Doneva M, Börnert P, Eggers H, Stehning C, Sénégas J, Mertins A. Compressed sensing reconstruction for magnetic resonance parameter mapping. *Magn. Reson. Med.* 2010; **64**: 1114–20. doi: https://doi.org/10.1002/mrm.22483
101. Fessler JA. Optimization methods for Mr image reconstruction. *arXiv preprint arXiv* 2019;, . **035101**903.
102. Lundervold AS, Lundervold A. An overview of deep learning in medical imaging focusing on MRI. *Z Med Phys* 2019; **29**: 102–27. doi: https://doi.org/10.1016/j.zemedi.2018.11.002
103. Küstner T, Liebgott A, Mauch L, Martirosian P, Bamberg F, Nikolaou K, et al. Automated reference-free detection of motion artifacts in magnetic resonance images. *MAGMA* 2018; **31**: 243–56. doi: https://doi.org/10.1007/s10334-017-0650-z
104. Sommer K, Saalbach A, Brosch T, Hall C, Cross NM, Andre JB. Correction of motion artifacts using a multiscale FullyConvolutional neural network. *AJNR Am J Neuroradiol* 2020; **41**: 416–23.
105. Zhu B, Liu JZ, Cauley SF, Rosen BR, Rosen MS. Image reconstruction by domain-transform manifold learning. *Nature* 2018; **555**: 487–92. doi: https://doi.org/10.1038/nature25988
106. Haskell MW, Cauley SF, Bilgic B, Hossbach J, Splitthoff DN, Pfeuffer J, et al. Network accelerated motion estimation and reduction (NAMER): Convolutional neural network guided retrospective motion correction using a separable motion model. *Magn Reson Med* 2019; **82**: 1452–61. doi: https://doi.org/10.1002/mrm.27771
107. Lee J, Han Y, Ryu J-K, Park J-Y, Ye JC. k-Space deep learning for reference-free epi ghost correction. *Magn Reson Med* 2019; **82**: 2299–313. doi: https://doi.org/10.1002/mrm.27896
108. Wang G, Ye JC, Mueller K, Fessler JA. Image reconstruction is a new frontier of machine learning. *IEEE Trans Med Imaging* 2018; **37**: 1289–96. doi: https://doi.org/10.1109/TMI.2018.2833635
109. Hammernik K, Klatzer T, Kobler E, Recht MP, Sodickson DK, Pock T, et al. Learning a variational network for reconstruction of accelerated MRI data. *Magn Reson Med* 2018; **79**: 3055–71. doi: https://doi.org/10.1002/mrm.26977
110. Kaur P, Singh G, Kaur P. A review of denoising medical images using machine learning approaches. *Curr Med Imaging Rev* 2018; **14**: 675–85. doi: https://doi.org/10.2174/1573405613666170428154156